



# Assessment of Bone Microarchitecture in Patients with Systemic Mastocytosis and its Association with Clinical and Biochemical Parameters of the Disease

Andre S. Franco<sup>1,4</sup> · Igor H. Murai<sup>1</sup> · Liliam Takayama<sup>1</sup> · Valeria F. Caparbo<sup>1</sup> · Luan L. Marchi<sup>2</sup> · Elvira D. R. P. Velloso<sup>2,3</sup> · Rosa M. R. Pereira<sup>1</sup>

Received: 14 March 2023 / Accepted: 30 May 2023 / Published online: 9 June 2023  
© The Author(s), under exclusive licence to Springer Science+Business Media, LLC, part of Springer Nature 2023

## Abstract

Patients with systemic mastocytosis (SM) are at high risk of bone deterioration. However, the evaluation of bone microarchitecture in this disease remains unclear. We aimed to assess bone microarchitecture in patients with SM. This was a cross-sectional study of 21 adult patients with SM conducted in a quaternary referral hospital in Sao Paulo, Brazil. A healthy, age-, weight-, and sex-matched cohort of 63 participants was used to provide reference values for bone microarchitecture, assessed by high resolution peripheral quantitative computed tomography (HR-pQCT). Total volumetric bone mineral density (vBMD), cortical vBMD, and cortical thickness at the radius were significantly lower in the control group compared with the SM group (all  $P < 0.001$ ). Patients with aggressive SM had significantly lower trabecular number (Tb.N) ( $P = 0.035$ ) and estimated failure load (F.load) ( $P = 0.032$ ) at the tibia compared with those with indolent SM. Handgrip strength was significantly higher in patients who had more Tb.N at the radius ( $\rho$ , 0.46;  $P = 0.036$ ) and tibia ( $\rho$ , 0.49;  $P = 0.002$ ), and lower who had more trabecular separation at the radius ( $\rho$ ,  $-0.46$ ;  $P = 0.035$ ) and tibia ( $\rho$ ,  $-0.52$ ;  $P = 0.016$ ). Strong and positive associations between F.load ( $\rho$ , 0.75;  $P < 0.001$ ) and stiffness ( $\rho$ , 0.70;  $P < 0.001$ ) at the radius, and between F.load at the tibia ( $\rho$ , 0.45;  $P = 0.038$ ) were observed with handgrip strength. In this cross-sectional study, aggressive SM was more susceptible to bone deterioration compared with indolent SM. In addition, the findings demonstrated that handgrip strength was associated with bone microarchitecture and bone strength.

**Keywords** Bone metabolism · HR-pQCT · Handgrip · Secondary osteoporosis · Tryptase

Rosa M. R. Pereira in memoriam.

✉ Andre S. Franco  
andre.franco@fm.usp.br

- <sup>1</sup> Rheumatology Division, Hospital das Clinicas HCFMUSP, Faculdade de Medicina da Universidade de Sao Paulo, Sao Paulo, Brazil
- <sup>2</sup> Service of Hematology, Transfusion and Cell Therapy and Laboratory of Medical Investigation in Pathogenesis and Directed Therapy in Onco-Immuno-Hematology (LIM-31) HCFMUSP, University of Sao Paulo Medical School, Sao Paulo, Brazil
- <sup>3</sup> Hospital Israelita Albert Einstein, Sao Paulo, Brazil
- <sup>4</sup> Faculdade de Medicina, FMUSP da Universidade de São Paulo, Av Dr Arnaldo, 455 – Reumatologia, 3º Andar, Sala 3193, Cerqueira César, Sao Paulo 01246-903, Brazil

## Introduction

Systemic mastocytosis (SM) is a rare hematological disease characterized by abnormal proliferation and accumulation of mast cells in various organs, mainly skin and bone marrow [1, 2]. Patients with SM are at high risk of bone deterioration and fragility fractures [3–6]. Although the mechanisms of bone loss in SM remain unknown [7, 8], it has been suggested that allergic mediators such as histamine and tryptase may act by increasing the activity of osteoclasts, leading to an increase in bone resorption [9, 10].

A comprehensive assessment of bone in SM is scarce, with dual-energy X-ray absorptiometry (DXA) being the most used method in previous studies [4–6]. In patients with SM, most fragility fractures may occur with normal bone mineral density (BMD), which requires assessment of bone-related quality parameters. DXA provides information on trabecular compartment based on lumbar spine textural

index (Trabecular Bone Score, TBS) [11], bone deformation (Bone Strain Index) [12], and bone cross-sectional geometry (Hip Structural Analysis) [13]. However, volumetric evaluation of bone tissue is not possible by DXA. In this context, high resolution peripheral quantitative computed tomography (HR-pQCT) emerges as an important technology that allows performing *in vivo* assessment of three dimensions high-definition bone structural measures [14]. Furthermore, the use of finite element models can estimate biomechanical properties of the tissue [14].

The objective of this study was to evaluate bone microarchitecture and bone strength using HR-pQCT in patients with SM, and their associations with clinical and biochemical parameters of the disease.

## Methods

This was a cross-sectional study in which patients with SM underwent a comprehensive evaluation of bone and were compared with a cohort of healthy individuals. The study was approved by the ethics committee of the Hospital das Clinicas of the School of Medicine of the University of Sao Paulo (#19821519.0.0000.0068, date of approval September 4, 2019) and all the patients provided written informed consent before participation.

### Participants

Patients with SM who fulfilled the WHO 2016 criteria [15] were recruited from Outpatient Hematology Clinic of the Hospital das Clinicas of the University of Sao Paulo, and were referred to the Rheumatology Division of the same institution for evaluation of bone parameters. Our institution is a public quaternary referral teaching hospital responsible for high complexity care. Patients were enrolled from October 2020 to June 2022, and the final analysis was in June 2022. To provide reference values for all measurements, we included a group of healthy adult participants whose data were obtained from a cohort who have participated in studies by our research group aimed to establish age-related reference curves for bone microarchitecture and strength [16, 17]. The control group was matched by age, weight, and sex in a ratio of 1:3.

### Outcomes

#### HR-pQCT

The primary outcome was bone microarchitecture assessed by HR-pQCT. The distal radius and distal tibia were scanned using a first-generation HR-pQCT scanner (XtremeCT I, Scanco Medical AG, Brüttisellen, Switzerland). The

measurements included 110 slices, corresponding to a 9.02 mm scan area (voxel size of 82  $\mu\text{m}$ ), positioned 9.5 mm and 22.5 mm proximal to the reference line for the distal radius and distal tibia, respectively. The variables measured were volumetric BMD (vBMD), structural parameters, and cortical porosity.

#### Finite Element Models

Finite element models were performed to estimate bone strength from HR-pQCT measurements using a specific software (Finite Element software v. 1.13, Scanco Medical AG, Switzerland). Models of the distal radius and distal tibia were generated directly from the HR-pQCT images (Image Processing Language and Finite Element Extension (IPLFE), Scanco Medical AG, Switzerland). The parameters obtained were estimated failure load (F.Load) and stiffness.

#### DXA

BMD Z-score and T-score at the lumbar spine, total hip, and femoral neck were measured using a DXA device (Lunar iDXA, GE Healthcare, Madison, WI).

TBS was assessed by the software TBS iNsite® version 2.1 (Medimaps, Bordeaux, France). It was analyzed as the mean value of the measurements of the L1–L4 vertebrae in the same region as the DXA images of the lumbar spine.

Vertebral fracture assessment (VFA) was obtained by lateral DXA scanning of the T4–L4 vertebrae. Assessments of vertebral fractures were performed using the method described by Genant et al. [18].

#### Handgrip Strength

Handgrip strength was assessed to obtain the maximum isometric strength of the dominant hand using a hydraulic hand dynamometer (SAEHAN SH5001, Saehan Corp.). Measurements were obtained with the participants in the sitting position and elbow flexed at 90°, and all assessments were performed by the same trained technician.

#### Biochemical Disease-related Markers

Quantification of KIT D816V mutation was performed by digital polymerase chain reaction (dPCR) [19]. Genomic DNA was obtained from peripheral blood leukocyte buttons collected in an EDTA tube. DNA extraction was performed using the QIAamp DNA Midi Kit (Qiagen, Ger) using  $5 \times 10^6$  cells, and the concentration of the obtained DNA was measured on the NanoDrop 2000 spectrophotometer (Thermo Fisher, USA). The search for the D816V mutation by dPCR was performed with 50 ng of genomic DNA using the QuantStudio™ 3D dPCR mastermix V2 (Thermo Fisher,

USA), and the Kit\_1314 assay (ID Hs000000039\_rm), according to the manufacturer's protocol. QuantStudio™ 3D dPCR AnalysisSuit software was used for the analysis of the results.

Serum tryptase levels were measured by fluorimetric immunoassay, with reference values between 1 and 15 µg/L and values greater than 20 µg/L was considered as a minor criterion for systemic mastocytosis.

### Mastocytosis Activity Score

Disease activity was measured using the Mastocytosis Activity Score [20]. This questionnaire was performed by the same trained physician.

### Bone Turnover Markers

Serum C-terminal telopeptide of type 1 collagen (CTX) and Procollagen type 1 N-terminal propeptide (P1NP) concentrations were determined by an automated electrochemiluminescence system (E411; Roche Diagnostics, Mannheim, Germany). Serum CTX and P1NP limits of detection were 10 ng/L and 5 mg/L, respectively.

### Statistical Analysis

Data are presented as mean  $\pm$  SD or median (IQR) and estimated difference between groups with 95% CI for continuous variables and as percentages for categorical variables. We used mixed models assuming group as fixed factor and subjects as a random factor to compare patients with SM and healthy individuals. Subgroup analyses using the Mann–Whitney U test were performed to compare patients with aggressive SM (aSM) and indolent SM (iSM). Spearman rank correlation ( $\rho$ ) was used to measure the associations between handgrip strength and disease-related markers with bone parameters. Percentages were compared between groups using Fisher's exact test. All tests were 2-sided and the significance level was set to  $\alpha=0.05$ . Statistical analyses were performed using SAS version 9.4 (SAS Institute, Cary, NC).

## Results

### Patients

Of 30 patients assessed for eligibility in the SM group, 21 were eligible and included in the study. Of the 9 patients not included, 3 died before the assessments, 2 had cutaneous mastocytosis, 2 refused to participate, 1 did not have a confirmed diagnosis, and 1 did not have personal contact in our medical record. Of the 21 patients, 3 (14.3%) were

men (Table 1), 15 (71.4%) had iSM, 6 (28.6%) had aSM, 6 (28.6%) had low bone mass, and 3 (14.3%) had osteoporosis (Table 2). No significant differences between the control group and the SM group were observed for age, weight, body mass index, sex, and race (Table 1).

### Primary Outcome

Total vBMD (difference,  $-61.0$  mgHA/cm<sup>3</sup> [95% CI  $-91.3$  to  $-30.7$ ];  $P<0.001$ ) and cortical vBMD (difference,  $-76.0$  mgHA/cm<sup>3</sup> [95% CI  $-110.1$  to  $-42.0$ ];  $P<0.001$ ) at the radius were significantly lower in the control group compared with the SM group (Table 1). In addition, cortical thickness at the same bone site significantly differed between the control group and the SM group (difference,  $-0.27$  mm [95% CI  $-0.36$  to  $-0.17$ ];  $P<0.001$ ) (Table 1). No significant differences between the groups were observed for any other bone microarchitecture parameters.

### Secondary Outcomes

Stiffness and F.load at the radius and tibia did not significantly differ between the groups. BMD Z-score at the lumbar spine was significantly lower in the SM group compared with the control group (difference,  $-0.68$  [95% CI,  $-1.36$  to  $-0.01$ ];  $P=0.047$ ) (Table 1). The SM group had significantly more vertebral fractures compared with the control group (14.3% vs. 0%,  $P=0.014$ ) (Table 1). No other significant differences were observed in BMD Z-score, T-score, and TBS (Table 1).

### Subgroup Analyses and Associations Between Handgrip Strength and Disease-related Markers with Bone Parameters

Subgroup analyses demonstrated that aSM group had significantly lower trabecular number (Tb.N) (difference,  $-0.56$  1/mm [95% CI  $-1.04$  to  $-0.07$ ];  $P=0.035$ ) (Fig. 1A) and F.load (difference,  $-1269.0$  N [95% CI  $-3417.0$  to  $-173.0$ ;  $P=0.032$ ) at the tibia compared with iSM group (Fig. 1B). No significant differences were observed for the other parameters of bone microarchitecture, bone strength, TBS, and VFA (Table 2). Handgrip strength, biochemical disease-related markers, disease activity, and serum bone turnover markers did not significantly differ between the aSM and the iSM (Table 2).

Handgrip strength was significantly higher in patients who had more Tb.N at the radius ( $\rho$ , 0.46, [95% CI 0.02–0.74];  $P=0.036$ ) (Fig. 2A) and tibia ( $\rho$ , 0.49, [95% CI 0.06–0.76];  $P=0.002$ ) (Fig. 2B), and lower who had more trabecular separation (Tb.Sp) at the radius ( $\rho$ ,  $-0.46$ , [95% CI  $-0.74$  to  $-0.03$ ];  $P=0.035$ ) (Fig. 2C) and tibia ( $\rho$ ,  $-0.52$ , [95% CI  $-0.77$  to  $-0.10$ ];  $P=0.016$ ) (Fig. 2D). Also, handgrip

**Table 1** Characteristics of participants and comparisons between control group and systemic mastocytosis (SM) group

Variable	Control group (n=63)	SM group (n=21)	Estimated Difference (95% CI)	P value
Age, y	46.9 ± 12.6	47.3 ± 13.1	- 0.44 (- 6.83 to 5.95)	0.8907
Weight, kg	68.8 ± 12.7	71.7 ± 18.6	- 2.84 (- 10.0 to 4.37)	0.4351
Body mass index, kg/m <sup>2</sup>	27.1 ± 4.5	27.8 ± 6.8	- 0.77 (- 3.38 to 1.84)	0.5588
Sex, No. (%)				
Women	54 (85.7)	18 (85.7)	-	> 0.999
Men	9 (14.3)	3 (14.3)		
Race, No. (%)				
White	52 (82.5)	19 (90.5)	-	0.5020
Black	11 (17.5)	2 (9.5)		
Coexisting diseases, No. (%)				
Obesity	14 (22.2)	3 (14.3)	-	0.5422
Hypertension	4 (6.3)	3 (14.3)		0.3591
Diabetes	1 (1.6)	2 (9.5)		0.1528
Tobacco-smoking	12 (19.0)	3 (14.3)	-	0.7512
Medications, No. (%)				
Cytoreductive therapy	0 (0)	4 (19.0)	-	0.0031
Glucocorticoid	0 (0)	7 (33.3)		< 0.0001
Antihistaminic	0 (0)	18 (85.7)		< 0.0001
Radius bone microarchitecture				
Tt.vBMD, mgHA/cm <sup>3</sup>	304.9 ± 59.2	365.9 ± 64.0	- 61.01 (- 91.31 to - 30.71)	0.0001
Tb.vBMD, mgHA/cm <sup>3</sup>	165.9 ± 42.7	155.8 ± 41.7	- 10.14 (- 11.15 to 31.43)	0.3463
Ct.vBMD, mgHA/cm <sup>3</sup>	853.6 ± 73.9	929.6 ± 44.4	- 76.02 (- 110.08 to - 41.97)	< 0.0001
BV/TV	0.138 ± 0.035	0.130 ± 0.035	0.008 (- 0.009 to 0.026)	0.3528
Tb.N, 1/mm	1.95 ± 0.33	1.82 ± 0.38	0.13 (- 0.04 to 0.31)	0.1243
Tb.Th, mm	0.070 ± 0.011	0.075 ± 0.028	- 0.004 (- 0.013 to 0.004)	0.3340
Tb.Sp, mm	0.457 ± 0.104	0.536 ± 0.309	- 0.078 (- 0.167 to 0.011)	0.0833
Ct.Th, mm	0.67 ± 0.18	0.94 ± 0.21	- 0.27 (- 0.36 to - 0.17)	< 0.0001
Tibia bone microarchitecture				
Tt.vBMD, mgHA/cm <sup>3</sup>	296.4 ± 59.7	307.4 ± 58.7	- 10.97 (- 40.77 to 18.82)	0.4657
Tb.vBMD, mgHA/cm <sup>3</sup>	153.6 ± 38.9	159.3 ± 49.4	- 5.62 (- 26.54 to 15.29)	0.5941
Ct.vBMD, mgHA/cm <sup>3</sup>	905.8 ± 54.0	900.9 ± 60.9	4.92 (- 23.04 to 32.88)	0.7273
BV/TV	0.128 ± 0.032	0.133 ± 0.041	- 0.004 (- 0.022 to 0.013)	0.5950
Tb.N, 1/mm	1.69 ± 0.35	1.79 ± 0.35	- 0.10 (- 0.28 to 0.07)	0.2526
Tb.Th, mm	0.076 ± 0.014	0.075 ± 0.022	0.001 (- 0.007 to 0.009)	0.7600
Tb.Sp, mm	0.542 ± 0.140	0.505 ± 0.119	0.037 (- 0.031 to 0.105)	0.2781
Ct.Th, mm	1.18 ± 0.30	1.24 ± 0.34	- 0.06 (- 0.21 to 0.10)	0.4458
Radius cortical porosity, %	1.88 ± 1.21	1.72 ± 1.09	0.15 (- 0.44 to 0.74)	0.6115
Tibia cortical porosity, %	4.15 ± 1.90	4.37 ± 2.60	- 0.22 (- 1.27 to 0.82)	0.6733
Radius estimated bone strength				
Stiffness, kN/mm	76.8 ± 20.5	81.5 ± 24.2	- 4.64 (- 15.41 to 6.14)	0.3943
F.load, N	3685.5 ± 993.0	3862.8 ± 1139.7	- 177.29 (- 693.94 to 339.35)	0.4967
Tibia estimated bone strength				
Stiffness, kN/mm	204.6 ± 50.9	213.9 ± 67.8	- 9.32 (- 37.15 to 18.51)	0.5073
F.load, N	9717.6 ± 2351.0	10,156.6 ± 3051.1	- 439.1 (- 1712.0 to 833.9)	0.4946
BMD Z-score				
Lumbar spine	+ 0.2 ± 1.2	- 0.5 ± 1.8	0.68 (0.01 to 1.36)	0.0474
Total hip	+ 0.1 ± 0.9	+ 0.4 ± 1.4	- 0.28 (- 0.81 to 0.26)	0.3061
Femoral neck	+ 0.1 ± 1.0	0.0 ± 1.3	0.12 (- 0.41 to 0.65)	0.6562
BMD T-score				
Lumbar spine	- 0.5 ± 1.2	- 0.8 ± 1.8	0.28 (- 0.41 to 0.98)	0.4187

Table 1 (continued)

Variable	Control group (n=63)	SM group (n=21)	Estimated Difference (95% CI)	P value
Total hip	-0.3 ± 1.0	+0.1 ± 1.5	-0.47 (-1.05 to 0.12)	0.1173
Femoral neck	-0.5 ± 1.1	-0.5 ± 1.4	-0.08 (-0.68 to 0.52)	0.7925
TBS L1-L4	1.370 ± 0.119	1.377 ± 0.120	-0.007 (-0.069 to 0.054)	0.8142
VFA T4-L4, No. (%)	0 (0)	3 (14.3)	-	0.0140

Data are expressed as mean ± SD or No. of patients (%)

*BMD* bone mineral density, *BV/TV* trabecular bone volume fraction, *Ct.Th* cortical thickness, *Ct.vBMD* cortical bone mineral density, *F.load* estimated failure load, *N* Newton, *Tb.N* trabecular number, *Tb.Sp* trabecular separation, *Tb.Th* trabecular thickness, *Tb.vBMD* trabecular volumetric bone mineral density, *Tt.vBMD* total volumetric bone mineral density, *TBS* trabecular bone score, *VFA* vertebral fracture assessment

strength was strongly and positively associated with *F.load* ( $\rho$ , 0.75, [95% CI 0.46–0.89];  $P < 0.001$ ) (Fig. 3A) and stiffness ( $\rho$ , 0.70, [95% CI 0.37–0.87];  $P < 0.001$ ) (Fig. 3B) at the radius, and with *F.load* at the tibia ( $\rho$ , 0.45, [95% CI 0.02–0.74];  $P = 0.038$ ) (Fig. 3C).

Serum tryptase levels were significantly and negatively associated with *F.load* at the radius ( $\rho$ , -0.46, [95% CI, -0.74 to -0.01];  $P = 0.040$ ) (Fig. 3D). No significant associations were observed between the age of the patients, the allele burden of the *KIT* D816V mutation, Mastocytosis Activity Score, and TBS with bone parameters and with handgrip strength.

## Discussion

In this cross-sectional study, we found that SM group significantly differ in some bone structural measurements when compared with healthy individuals. Trabecular compartments of the tibia were lower in the aSM, possibly causing a reduction in bone strength. In addition, handgrip strength was associated with trabecular parameters and bone strength of the radius and tibia. To our knowledge, this is the first study to comprehensively assess bone using HR-pQCT in SM.

In SM, the accumulation of mast cells increases the levels of histamine, tryptase and cytokines, which may have a role in bone impairment. Approximately 0.5% of all causes of osteoporosis are derived from SM [10]. However, in young males, SM is responsible for 6% of secondary osteoporosis. Cohort studies show that patients with SM have 20–28% osteoporosis and 28–37% fragility fracture [5–8, 21].

Degboé et al. showed that bone marrow tryptase levels are associated with fragility fractures [6]. Our study did not show this relationship, but we observed an inverse association between serum tryptase levels and *F.load* at the radius.

Studies with knockout rodents of the enzyme histamine decarboxylase showed a lower number of osteoclasts and an increase in bone formation, indicating the role of this mediator on bone metabolism [22]. Moreover, histamine is involved in activating the RANK-RANKL system, which stimulates osteoclastogenesis [23]. Finally, in vitro studies using H1 and H2 histamine receptor antagonists showed a reduction in the number of osteoclasts [24].

In our study, although some cortical compartments of the radius were higher in SM, lumbar spine Z-score were lower compared with the control group, suggesting that SM may decrease the trabecular bone to a greater extent. Subgroup analyses may support this observation, as the *Tb.N* at the tibia was more affected in the aSM, possibly leading to a reduction in the *F.load*. Our findings corroborate with other studies that show impaired BMD at the lumbar spine and vertebral fractures in patients with SM when compared with healthy individuals [8, 10, 25].

Handgrip strength is a low-cost, easy-to-implement method for accurately measuring muscle strength. A recent study demonstrated that handgrip strength was associated with bone erosion assessed by HR-pQCT in patients with rheumatoid arthritis [26]. Our findings showed associations between handgrip strength and *Tb.N* and *Tb.Sp* at both radius and tibia, in addition to strong correlations with biomechanical parameters, suggesting that this method may be useful for estimating bone deterioration in SM.

The limitations of this study include the small sample size and single-center observational design. Although the SM is a rare disease, with about one case in sixty thousand, all patients treated at our referral hospital were included in the sample. In addition, the high mortality rate due to the poor prognosis of aSM resulted in the death of many patients before enrollment in the study, which limited the sample size of this subgroup and precluded the use of multiple regression analysis models to investigate the relationships between outcomes and variables that could represent a bias,

**Table 2** Comparisons between aggressive systemic mastocytosis (aSM) group and indolent systemic mastocytosis (iSM) group

Variable	aSM group (n=6)	iSM group (n=15)	Estimated difference (95% CI)	P value
Age, y	57.3 (32.6–61.3)	47.9 (39.6–55.8)	6.8 (– 17.9 to 31.3)	0.3706
Weight, kg	63.9 (58.1–81.1)	73.3 (58.4–82.5)	– 4.7 (– 25.6 to 16.2)	0.7853
Body mass index, kg/m <sup>2</sup>	27.9 (25.5–32.9)	25.0 (22.6–30.3)	2.7 (– 4.2 to 9.6)	0.2933
Sex, No. (%)				
Women	6 (100)	12 (80.0)	–	0.5263
Men	0 (0)	3 (20.0)		
Race, No. (%)				
White	6 (100)	13 (86.7)	–	> 0.9999
Black	0 (0)	2 (13.3)		
Coexisting diseases, No. (%)				
Obesity	2 (33.3)	4 (26.7)	–	> 0.9999
Hypertension	0 (0)	1 (6.7)		> 0.9999
Diabetes	0 (0)	2 (13.3)		> 0.9999
Tobacco-smoking	2 (33.3)	1 (2.1)	–	0.1842
Medications, No. (%)				
Cytoreductive therapy	4 (66.7)	0 (0)	–	0.0025
Glucocorticoid	3 (50)	4 (26.7)		0.3544
Antihistaminic	6 (100)	12 (80)		0.5263
Radius bone microarchitecture				
Tt.vBMD, mgHA/cm <sup>3</sup>	381.0 (372.5–400.9)	353.8 (316.6–396.5)	23.4 (– 17.9 to 64.7)	0.3706
Tb.vBMD, mgHA/cm <sup>3</sup>	143.9 (106.3–160.7)	148.9 (135.5–190.1)	6.3 (– 40.2 to 52.8)	0.4137
Ct.vBMD, mgHA/cm <sup>3</sup>	955.7 (910.1–978.2)	922.9 (886.3–948.5)	30.3 (– 26.6 to 87.2)	0.1194
BV/TV	0.120 (0.089–0.134)	0.124 (0.113–0.158)	– 0.005 (– 0.043 to 0.033)	0.4361
Tb.N, 1/mm	1.78 (1.70–1.85)	1.94 (1.84–2.04)	– 0.14 (– 0.31 to 0.03)	0.1192
Tb.Th, mm	0.069 (0.052–0.091)	0.063 (0.060–0.091)	0.013 (– 0.018 to 0.044)	0.9067
Tb.Sp, mm	0.486 (0.463–0.537)	0.438 (0.422–0.483)	0.043 (– 0.025 to 0.111)	0.1388
Ct.Th, mm	1.00 (0.87–1.31)	0.91 (0.76–0.99)	0.04 (– 0.30 to 0.38)	0.2584
Tibia bone microarchitecture				
Tt.vBMD, mgHA/cm <sup>3</sup>	303.8 (234.5–310.8)	312.0 (264.1–344.3)	– 7.6 (– 75.0 to 59.8)	0.3706
Tb.vBMD, mgHA/cm <sup>3</sup>	133.8 (105.2–154.1)	151.9 (133.0–203.9)	– 15.3 (– 63.4 to 32.8)	0.3305
Ct.vBMD, mgHA/cm <sup>3</sup>	884.9 (832.4–973.1)	920.8 (860.8–943.6)	– 4.8 (– 116.1 to 106.5)	0.8456
BV/TV	0.112 (0.088–0.128)	0.127 (0.111–0.170)	– 0.013 (– 0.053 to 0.027)	0.2928
Tb.N, 1/mm	1.43 (1.38–1.94)	2.00 (1.57–2.15)	– 0.56 (– 1.04 to – 0.07)	0.0355
Tb.Th, mm	0.065 (0.055–0.095)	0.069 (0.061–0.085)	– 0.003 (– 0.034 to 0.028)	0.7258
Tb.Sp, mm	0.602 (0.452–0.662)	0.423 (0.406–0.567)	0.138 (– 0.033 to 0.309)	0.0565
Ct.Th, mm	1.12 (0.91–1.31)	1.26 (1.09–1.31)	– 0.06 (– 0.40 to 0.28)	0.4584
Radius cortical porosity, %	1.63 (0.62–2.71)	1.43 (0.70–2.71)	0.79 (– 1.00 to 2.58)	> 0.9999
Tibia cortical porosity, %	4.49 (2.13–6.08)	2.69 (2.31–6.62)	0.008 (– 0.010 to 0.026)	> 0.9999
Radius estimated bone strength				
Stiffness, kN/mm	75.36 (70.90–81.09)	76.23 (65.62–89.76)	0.16 (– 12.9 to 13.2)	0.7261
F.load, N	3600.5 (3488.0–3814.2)	3513.6 (3135.1–4242.3)	34.8 (– 515.3 to 584.9)	0.7261
Tibia estimated bone strength				
Stiffness, kN/mm	178.14 (160.00–197.60)	202.59 (180.87–255.90)	– 15.1 (– 61.2 to 31.0)	0.0673
F.load, N	8379.9 (7666.2–9468.8)	9798.7 (8554.7–12,126.0)	– 1269.0 (– 3417.0 to – 173.0)	0.0323
BMD Z-score				
Lumbar spine	– 0.5 (– 2.7–0.9)	– 0.6 (– 1.0–0.2)	0.0 (– 2.7 to 2.7)	> 0.9999
Total hip	0.3 (– 0.9–0.8)	0.3 (– 0.6–1.9)	0.0 (– 2.2 to 2.2)	0.6623
Femoral neck	0.2 (– 0.4–0.4)	– 0.2 (– 1.1–0.5)	0.4 (– 1.7 to 2.5)	0.9650
BMD T-score				
Lumbar spine	– 0.9 (– 2.3– – 0.3)	– 0.7 (– 1.3–0.2)	– 0.1 (– 1.8 to 1.6)	0.7258

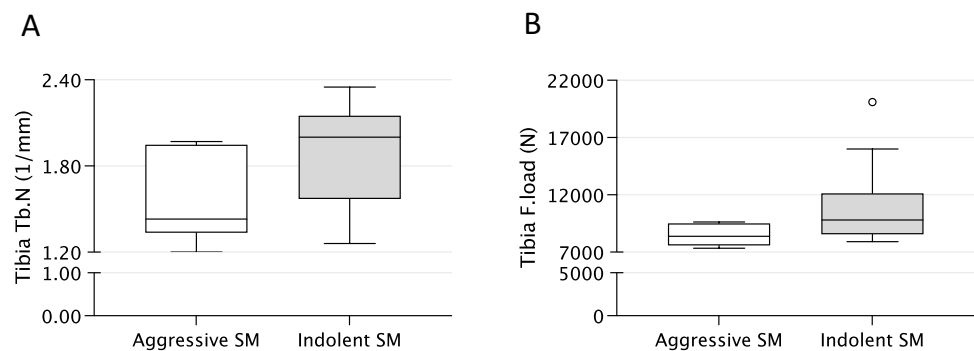
Table 2 (continued)

Variable	aSM group (n=6)	iSM group (n=15)	Estimated difference (95% CI)	P value
Total hip	-0.1 (-0.3-0.0)	0.1 (-0.5-1.9)	-0.2 (-1.7 to 1.3)	0.4845
Femoral neck	-0.1 (-0.5-0.0)	-0.6 (-1.5-0.4)	-0.5 (-0.8 to 1.8)	>0.9999
TBS L1-L4	1.387 (1.218-1.467)	1.388 (1.357-1.443)	0.064 (-0.136 to 0.264)	0.7104
VFA T4-L4, No. (%)	1 (16.7)	2 (13.3)	-	>0.9999
Biochemical disease-related markers and disease activity				
<i>KIT</i> D816V mutation, VAF (%)	2.73 (0.38-4.98)	0.56 (0.15-1.83)	1.80 (-1.58 to 5.19)	0.1736
Tryptase, µg/L	76.1 (33.6-131.0)	45.8 (20.6-108.0)	19.1 (-68.4 to 106.6)	0.3641
MAS	12.5 (11.0-15.0)	7.0 (1.0-16.0)	4.0 (-4.0 to 12.0)	0.6492
Handgrip strength, N	19.4 (18.6-22.7)	21.3 (17.8-30.0)	-1.3 (-7.5 to 4.9)	0.3915
Bone turnover markers, ng/mL				
CTX	0.38 (0.11-0.84)	0.33 (0.27-0.60)	0.11 (-0.44 to 0.67)	0.9070
P1NP	58.3 (22.5-70.9)	57.0 (41.5-88.3)	9.9 (-31.8 to 51.6)	0.7853

Data are expressed as median (IQR) or No. of patients (%)

*BMD* bone mineral density, *BV/TV* trabecular bone volume fraction, *Ct.Th* cortical thickness, *Ct.vBMD* cortical bone mineral density, *CTX* C-terminal telopeptide of type 1 collagen, *F.load* estimated failure load, *MAS* mastocytosis activity score, *N* Newton, *P1NP* procollagen type 1 N-terminal propeptide, *Tb.N* trabecular number, *Tb.Sp* trabecular separation, *Tb.Th* trabecular thickness, *Tb.vBMD* trabecular volumetric bone mineral density, *Tt.vBMD* total volumetric bone mineral density, *TBS* trabecular bone score, *VAF* variant allele frequency, *VFA* vertebral fracture assessment

**Fig. 1** Subgroup analyses. **A** Trabecular number (Tb.N) at the tibia. **B** Estimated failure load (F.load) at the tibia. Boxes represent median and interquartile range with whiskers extending to the highest and lowest values within 1.5 IQR of the 25th and 75th percentiles. Outliers are represented with dots



particularly for the handgrip findings. Furthermore, we were unable to use bone marrow biopsies for histomorphometric analysis, which could elucidate mechanisms of bone loss.

Despite the challenges of conducting a study on a rare disease, our findings will contribute to the understanding of this disease and potential treatment options. The findings should be considered exploratory and hypothesis-generating. Further studies should confirm our results.

## Conclusion

Among patients with SM, bone microarchitecture and bone strength were more affected in aSM compared with iSM. Associations between handgrip strength and parameters of bone microarchitecture and bone biomechanical were also observed, suggesting that handgrip strength may be a feasible method to estimate bone deterioration in the SM.

**Fig. 2** Associations between handgrip strength and bone microarchitecture. **A** Trabecular number (Tb.N) at the radius. **B** Tb.N at the tibia. **C** Trabecular Separation (Tb.Sp) at the radius. **D**, Tb.Sp at the tibia

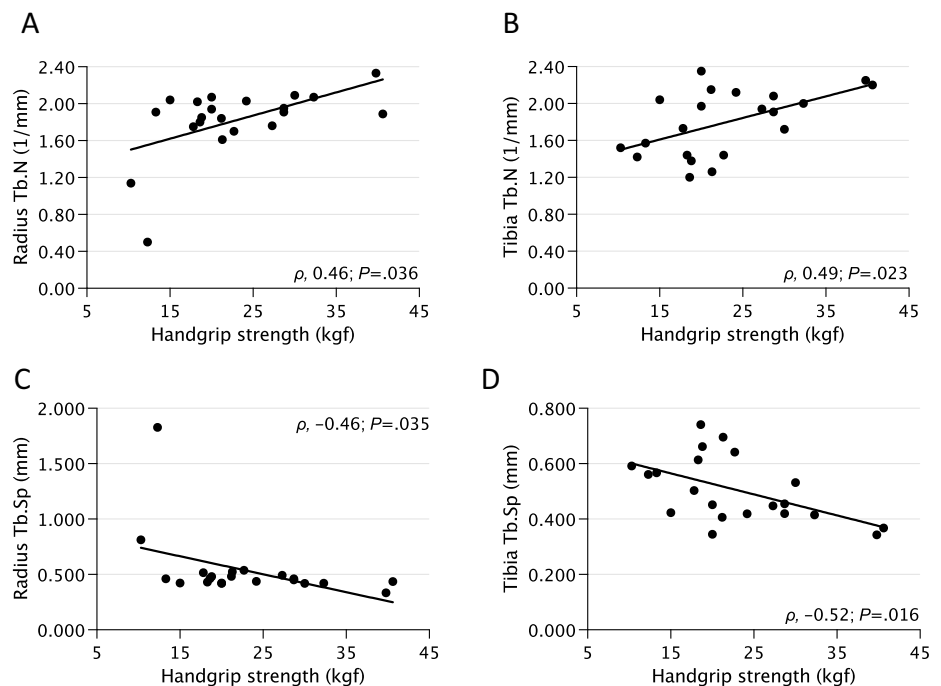
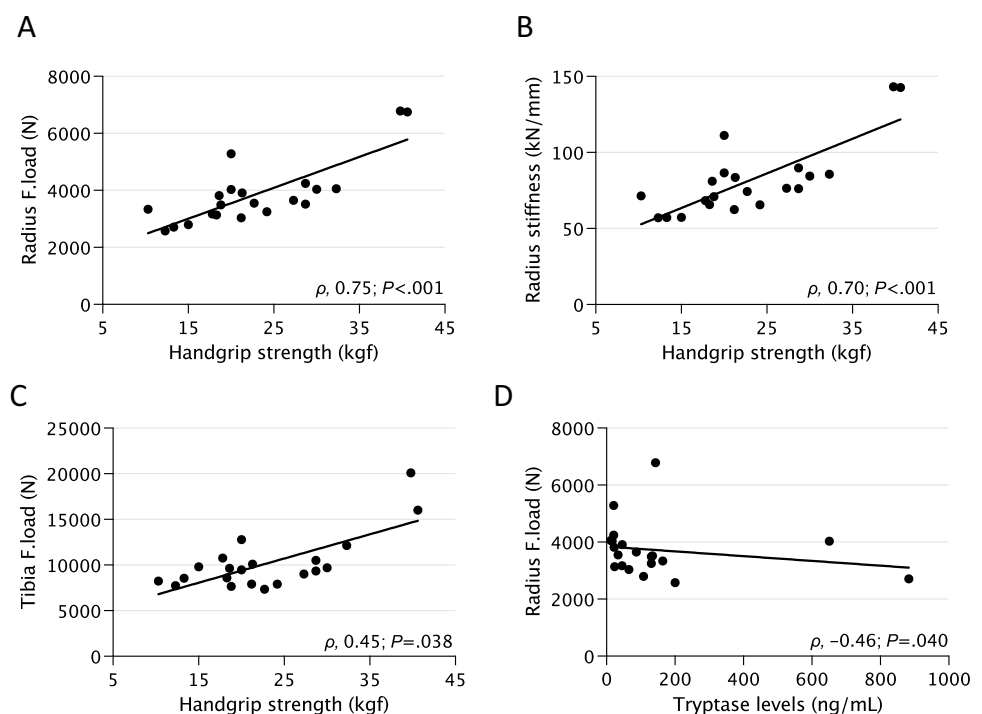


**Fig. 3** Associations between handgrip strength, serum tryptase levels and bone strength. **A** Estimated failure load (F.load) at the radius. **B** Stiffness at the radius. **C** F.load at the tibia. **D** F.load at the radius



**Author Contributions** ASF had full access to all of the data in the study and take responsibility for the integrity of the data and the accuracy of the data analysis. Concept and design: ASF, IHM, EDRPV, RMRP. Acquisition, analysis, and interpretation: All authors. Drafting of the manuscript: ASF, IHM. Critical revision of the manuscript for important intellectual content: All authors. Statistical analysis: ASF, IHM, EDRPV. Obtained funding: EDRPV, RMRP. Supervision: EDRPV, RMRP. Administrative, technical, or material support: LT, VFC. Dra Luciana Nardinelli (Laboratory of Tumor Biology of Hospital das

Clínicas da FMUSP for performing the dPCR KIT D816V studies) and Dr. Elaine Aparecida Rosseto (Clinical Laboratory of Hospital Israelita Albert Einstein) for performing tryptase tests. The authors are thankful to all the patients who participated in this study. All the individuals described in this section received no compensation for their participation in the study.

**Funding** This study was supported by Sao Paulo Research Foundation (FAPESP) (grants 19/24782-4).



## Declarations

**Conflict of interest** Andre S. Franco, Igor H. Murai, Liliam Takayama, Valeria F. Caparbo, Luan L. Marchi, Elvira D. R. P. Velloso, and Rosa M. R. Pereira declare that they have no conflict of interest.

**Role of the Funder/Sponsor** The funders had no role in the design and conduct of the study; collection, management, analysis, and interpretation of the data; preparation, review, or approval of the manuscript; and decision to submit the manuscript for publication.

**Human and Animal Rights and Informed Consent** The study was approved by the ethics committee of the Hospital das Clínicas of the School of Medicine of the University of Sao Paulo (#19821519.0.0000.0068, date of approval September 4, 2019) and all the patients provided written informed consent before participation.

## References

- Pardanani A (2021) Systemic mastocytosis in adults: 2021 Update on diagnosis, risk stratification and management. *Am J Hematol* 96:508–525
- Theoharides TC, Valent P, Akin C (2015) Mast cells, mastocytosis, and related disorders. *N Engl J Med* 373:163–172
- Broesby-Olsen S, Farkas DK, Vestergaard H, Hermann AP, Møller MB, Mortz CG, Kristensen TK, Bindsvlev-Jensen C, Sørensen HT, Frederiksen H (2016) Risk of solid cancer, cardiovascular disease, anaphylaxis, osteoporosis and fractures in patients with systemic mastocytosis: a nationwide population-based study. *Am J Hematol* 91:1069–1075
- Rossini M, Zanotti R, Bonadonna P, Artuso A, Caruso B, Schena D, Vecchiato D, Bonifacio M, Viapiana O, Gatti D, Senna G, Riccio A, Passalacqua G, Pizzolo G, Adami S (2011) Bone mineral density, bone turnover markers and fractures in patients with indolent systemic mastocytosis. *Bone* 49:880–885
- van der Veer E, van der Goot W, de Monchy JG, Kluijn-Nelemans HC, van Doornaal JJ (2012) High prevalence of fractures and osteoporosis in patients with indolent systemic mastocytosis. *Allergy* 67:431–438
- Degboé Y, Eischen M, Nigon D, Apoil PA, Mailhol C, Tournier E, Laurent C, Hanssens K, Hermine O, Paul C, Laroche M, Bulai-Livideanu C (2017) Prevalence and risk factors for fragility fracture in systemic mastocytosis. *Bone* 105:219–225
- Orsolini G, Viapiana O, Rossini M, Bonifacio M, Zanotti R (2018) Bone disease in mastocytosis. *Immunol Allergy Clin North Am* 38:443–454
- Rossini M, Zanotti R, Viapiana O, Tripi G, Orsolini G, Idolazzi L, Bonadonna P, Schena D, Escribano L, Adami S, Gatti D (2014) Bone involvement and osteoporosis in mastocytosis. *Immunol Allergy Clin North Am* 34:383–396
- Seitz S, Barvencik F, Koehne T, Priemel M, Pogoda P, Semler J, Minne H, Pfeiffer M, Zustin J, Püschel K, Eulenburg C, Schinke T, Amling M (2013) Increased osteoblast and osteoclast indices in individuals with systemic mastocytosis. *Osteoporos Int* 24:2325–2334
- Gehlen M, Schmidt N, Pfeifer M, Balasingam S, Schwarz-Eywill M, Maier A, Werner M, Siggelkow H (2021) Osteoporosis caused by systemic mastocytosis: prevalence in a Cohort of 8392 patients with osteoporosis. *Calcif Tissue Int* 109:685–695
- Hans D, Barthe N, Boutroy S, Pothuaud L, Winzenrieth R, Krieg MA (2011) Correlations between trabecular bone score, measured using anteroposterior dual-energy X-ray absorptiometry acquisition, and 3-dimensional parameters of bone microarchitecture: an experimental study on human cadaver vertebrae. *J Clin Densitom* 14:302–312
- Ulivieri FM, Rinaudo L (2022) The bone strain index: an innovative dual X-ray absorptiometry bone strength index and its helpfulness in clinical medicine. *J Clin Med* 11:2284–2296
- Ulivieri FM, Rinaudo L, Piodi LP, Barbieri V, Marotta G, Sciumè M, Grifoni FI, Cesana BM (2020) Usefulness of dual X-ray absorptiometry-derived bone geometry and structural indexes in mastocytosis. *Calcif Tissue Int* 107:551–558
- Fuller H, Fuller R, Pereira RM (2015) High resolution peripheral quantitative computed tomography for the assessment of morphological and mechanical bone parameters. *Rev Bras Reumatol* 55:352–362
- Valent P, Akin C, Metcalfe DD (2017) Mastocytosis: 2016 updated WHO classification and novel emerging treatment concepts. *Blood* 129:1420–1427
- Alvarenga JC, Fuller H, Pasoto SG, Pereira RM (2017) Age-related reference curves of volumetric bone density, structure, and biomechanical parameters adjusted for weight and height in a population of healthy women: an HR-pQCT study. *Osteoporos Int* 28:1335–1346
- Alvarenga JC, Caparbo VF, Domiciano DS, Pereira RMR (2022) Age-related reference data of bone microarchitecture, volumetric bone density, and bone strength parameters in a population of healthy Brazilian men: an HR-pQCT study. *Osteoporos Int* 33:1309–1321
- Genant HK, Wu CY, van Kuijk C, Nevitt MC (1993) Vertebral fracture assessment using a semiquantitative technique. *J Bone Miner Res* 8:1137–1148
- Greiner G, Gurbisz M, Ratzinger F, Witzeneder N, Simonitsch-Klupp I, Mitterbauer-Hohendanner G, Mayerhofer M, Müllauer L, Sperr WR, Valent P, Hoermann G (2018) Digital PCR: a sensitive and precise method for KIT D816V quantification in mastocytosis. *Clin Chem* 64:547–555
- Siebenhaar F, Sander B, Ho LHT, Ellrich A, Maurer M, Weller K (2018) Development and validation of the mastocytosis activity score. *Allergy* 73:1489–1496
- Guillaume N, Desoutter J, Chandesris O, Merlusca L, Henry I, Georjin-Lavialle S, Barete S, Hirsch I, Bouredji D, Royer B, Gruson B, Lok C, Sevestre H, Mentaverri R, Brazier M, Meynier J, Hermine O, Marolleau JP, Kamel S, Damaj G (2013) Bone complications of mastocytosis: a link between clinical and biological characteristics. *Am J Med* 126:75.e71–77
- Fitzpatrick LA, Buzas E, Gagne TJ, Nagy A, Horvath C, Ferencz V, Mester A, Kari B, Ruan M, Falus A, Barsony J (2003) Targeted deletion of histidine decarboxylase gene in mice increases bone formation and protects against ovariectomy-induced bone loss. *Proc Natl Acad Sci USA* 100:6027–6032
- Biosse-Duplan M, Baroukh B, Dy M, de Vernejoul MC, Saffar JL (2009) Histamine promotes osteoclastogenesis through the differential expression of histamine receptors on osteoclasts and osteoblasts. *Am J Pathol* 174:1426–1434
- Dobigny C, Saffar JL (1997) H1 and H2 histamine receptors modulate osteoclastic resorption by different pathways: evidence obtained by using receptor antagonists in a rat synchronized resorption model. *J Cell Physiol* 173:10–18
- Degboé Y, Eischen M, Apoil PA, Mailhol C, Dubreuil P, Hermine O, Paul C, Bulai Livideanu C, Laroche M (2019) Higher prevalence of vertebral fractures in systemic mastocytosis, but not in cutaneous mastocytosis and idiopathic mast cell activation syndrome. *Osteoporos Int* 30:1235–1241
- Figueiredo CP, Perez MO, Sales LP, Domiciano DS, Sampaio-Barros MM, Caparbo VF, Pereira RMR (2022) Lower hand grip in rheumatoid arthritis patients is associated with low finite element analysis using high resolution peripheral quantitative computed

tomography scan of the 2nd metacarpophalangeal joint. *Int J Rheum Dis* 25:1038–1045

**Publisher's Note** Springer Nature remains neutral with regard to jurisdictional claims in published maps and institutional affiliations.

Springer Nature or its licensor (e.g. a society or other partner) holds exclusive rights to this article under a publishing agreement with the author(s) or other rightsholder(s); author self-archiving of the accepted manuscript version of this article is solely governed by the terms of such publishing agreement and applicable law.